Chapter 2

FAST ELECTRONIC TRANSPORT AND COULOMB EXPLOSION IN MATERIALS IRRADIATED WITH ULTRASHORT LASER PULSES

Nadezhda M. Bulgakova[1], Razvan Stoian[2], Arkadi Rosenfeld[3], Ingolf V. Hertel[3,4], and Eleanor E.B. Campbell[5]

[1]Institute of Thermophysics SB RAS, 1 Lavrentyev Ave., 630090 Novosibirsk, Russia [2]Laboratoire TSI (UMR 5516 CNRS), Universite Jean Monnet, 10 rue Barrouin, 42000 Saint Etienne, France, [3]Max-Born-Institut für Nichtlineare Optik und Kurzzeitspektroskopie, Max-Born Str. 2a, D-12489 Berlin, Germany, [4]Department of Physics, Free University of Berlin, Amimallee 14, 14195 Berlin, Germany, [5]Department of Physics, Göteborg University, SE-41296 Göteborg, Sweden

1. INTRODUCTION

Ultrafast laser ablation of dielectrics and semiconductors proceeds through a sequence of physical processes such as nonlinear absorption, non-equilibrium effects related to electronic and vibrational excitations, and avalanche breakdown, generating dense, overcritical electron-hole plasmas during the action of the laser pulse. One of the most intriguing and complicated features of laser heating and ablation of dielectric materials is the strong temporal and spatial variation of the optical properties, ranging from a fully transparent, non-reflecting substance to a metal-like state. In dielectrics, metal-like behavior develops in a narrow surface layer. This results in strong localization of the energy coupling since the electron thermal conductivity is restricted to the high-density region. This aspect accounts for one of the main distinctions between metals and dielectrics under pulsed laser irradiation, the possibility of Coulomb explosion (CE) as an ablation mechanism alternative or additional to phase explosion.

Coulomb explosion is one of the electronic mechanisms of material removal from interfaces or surfaces sputtered by photons or charged particles (Fleischer, et al., 1965; Bitenskii et al., 1979; Schneider and Briere, 1996; Cheng and Gillaspy, 1997; Varel, et al., 1998; Stoian, et al., 2000a,

2000b, 2000c, 2002a; Henyk, et al., 2000a, 2000b; Vanagas, et al., 2003; Costache, et al. 2003; Costache and Reif, 2004). The occurrence of this particular phenomenon was intensely discussed during the last decades for various materials with radically different electronic properties. It has been postulated that CE can be exploited in different applications such as surface nanostructuring (Stoian, et al., 2002a; Vanagas, et al., 2003) and nanoparticle formation (Dong and Molian, 2004). Note that when referring to Coulomb explosion, we imply removal of at least several monolayers (Stoian, et al., 2000c; Bulgakova, et al., 2004a). We are not referring to electrostatic desorption, which is of a stochastic nature and results from localization of electronic excitation energy at specific atomic sites (Kanasaki and Tanimura, 2002). The main features of CE are the following. Energetic ions of different species, e.g., aluminum and oxygen in the case of ultrafast laser ablation of sapphire (Stoian, et al., 2000c), detected by time-of-flight mass spectrometry, have the same momenta but not the same energy. Also, doubly-charged ions have velocities twice as high as singly-charged ones. This indicates that the ions could be extracted and accelerated in the electric field generated in the target following a laser-induced neutrality breakdown. The electric field can be generated due to intensive electron photoemission, leading to accumulation of positive charge in a superficial target layer. Thus, *the concept of Coulomb explosion* is based on the fact that, due to photoemission, the irradiated surface gains a high positive charge, so that the repulsive force between ions exceeds the lattice binding strength, resulting in surface layer disintegration. An interesting CE aspect, in view of practical applications, is that the exploded material leaves behind a smooth, perfect surface that makes Coulomb explosion attractive for nanoscale applications (Stoian, et al., 2000c).

The present article gives an account of the underlying physical phenomena of the CE mechanism of laser ablation and presents a unified model to describe the processes that can influence the development and decay of charge accumulation on the surfaces of laser-irradiated materials of different classes (dielectrics, semiconductors, and metals). We will confine our considerations to gold, silicon, and sapphire as typical representatives of their classes.

2. EXPERIMENTAL EVIDENCE IN FAVOR OF LASER-INDUCED COULOMB EXPLOSION

The ultrashort pulse laser ablation of Al_2O_3 has been the subject of a large number of studies due to its useful mechanical, optical, and electrical properties. This material exhibits two completely different etch phases under laser irradiation (Tam, et al., 1989; Brand and Tam, 1990; Ashkenasi, et al.,

1997; Varel, et al., 1998; Stoian, et al., 2000a, 2000b, 2000c): a "gentle" ablation with material removal of a few nanometers per pulse and a "strong" ablation phase characterized by an order of magnitude higher ablation rate. "Gentle" ablation is characteristic for the irradiation regimes slightly above the ablation threshold and for a low number of laser shots irradiating the same surface area. Under the "gentle" ablation phase, the ablated material leaves behind an extremely smooth surface (sometimes even smoother than the initial state) (Fig. 1a). With increasing laser fluence and/or increasing number of shots, the "strong" ablation phase takes over and the irradiated surface begins to show the characteristics of "phase explosion" (Fig. 1b).

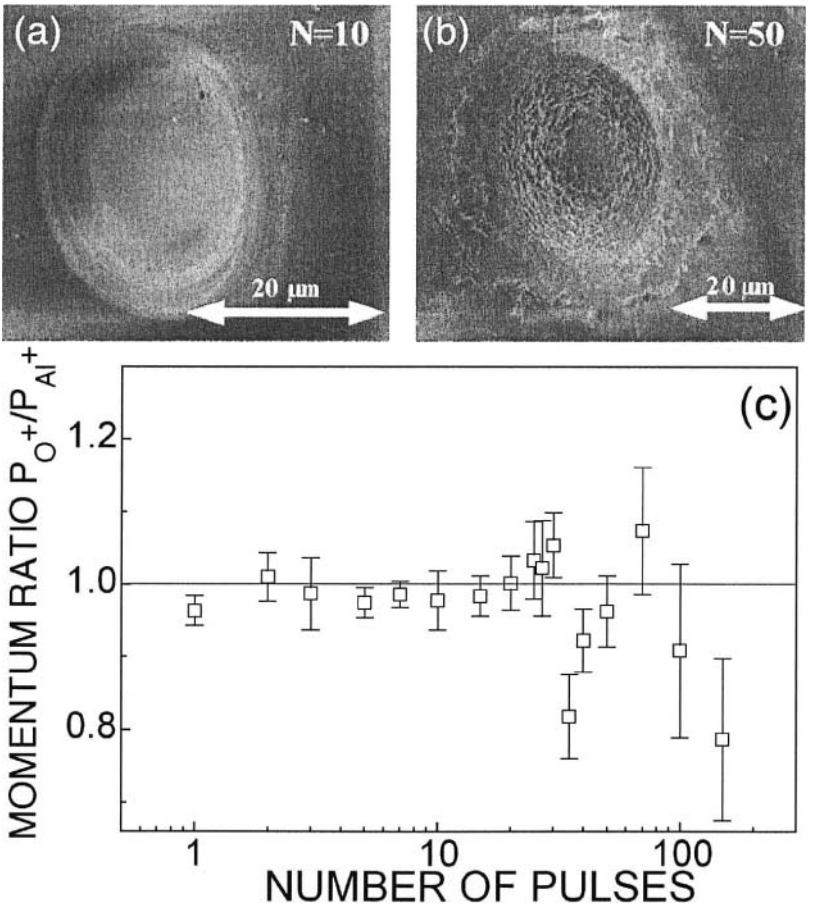

Figure 1. Transition from "gentle" (a) to "strong" (b) etch phase under ultrashort pulse laser ablation of Al_2O_3 (200 fs, 4 J/cm^2) with increasing number of shots. (c) Ratio of ion momenta, calculated from maxima of the velociy distributions. Reproduced from Stoian, et. al., 2000b.

Experimental evidence shows that under ultrafast irradiation of dielectric materials a significant component of the ablation products at intensities close to the material removal threshold is generated via a mechanism of electrostatic nature. We present below a short review of the experimental results.

The observed ionization degree and ion velocity distributions under the two etch phases differ considerably. Under gentle ablation, the ions, constituting the main component of the plume, have a clearly non-thermal nature exhibiting a most probable velocity of $\sim 2 \cdot 10^4$ m/s and a narrow angular velocity distribution directed along the normal to the irradiated targets. With the transition to the strong ablation stage, the ion velocity distributions become broader and slower, and thermal plasma ions ($\sim 1.2 \cdot 10^4$ m/s) are seen predominantly in the time-of-flight signals (Stoian, et al., 2000c). Moreover, ions of different species (Al^+ and O^+) observed under the gentle etch phase have mass-independent momenta (Fig. 1c), while on the transition to the strong phase they tend to have mass-independent quasi-equal energies (Stoian et al., 2002a, 2000c). These features indicate that, under gentle ablation, the ions are subjected to the action of a mass-independent acceleration mechanism, most probably due to a transient electric field generated in the target. The origin of the laser-induced neutrality breakdown is based on two main consequences of the interaction: a relatively high photoemission yield and a reduction of the transport properties for the laser-generated carriers. Even more striking is the difference in the behavior of F^+ and F^- ions, observed under barium fluoride ablation (Henyk, et al., 2000b), where the negative ions are retarded by the generated electric field.

3. CRITERION FOR COULOMB EXPLOSION

The occurrence of surface Coulomb explosion generating macroscopic material removal and high ion kinetic energies has been observed for dielectric materials, as mentioned above, while for semiconductors and metals the subject remains controversial (Gamaly, et al., 2002; Bulgakova, et al., 2005a). This raises the question: What processes are responsible for the CE occurrence or its inhibition? The answer to this question is based on a detailed study of the processes taking place in different types of laser-irradiated materials and their intricate interplay. Consequently, we introduce here a criterion for the occurrence of CE.

It is assumed that the electric field generated in the irradiated target can reach extremely high values so that the atomic bonds are broken and a surface layer of the material is disintegrated, resulting in the occurrence of Coulomb explosion. The estimation of the threshold electric field with respect to CE can be made by assuming that the electrostatic energy density

per individual atom exceeds a threshold value related to the required sublimation energy per atom. The threshold electric field can be approximated as $E_{th}\big|_{x=0} = \sqrt{2\Lambda_{at} n_0 / \varepsilon\varepsilon_0}$, where Λ_{at} is the sublimation energy per atom, n_0 is the lattice atomic density, and ε is the dielectric permittivity. For sapphire we obtain $E_{th} \sim 5 \cdot 10^{10}$ V/m, while for gold and silicon the estimated threshold electric fields are smaller, $2.76 \cdot 10^{10}$ and $2.65 \cdot 10^{10}$ V/m, respectively. This assumption is valid for the case of a cold lattice, roughly during femtosecond laser exposure. For longer pulses or longer times, one should take into account that the heated lattice atoms, having a higher vibrational energy, can escape from the surface with higher probability than the cold ones. Thus, thermal reduction of the threshold field can be expressed as $E_{th}\big|_{x=0} = \sqrt{2(\Lambda_{at} - 3kT_l) n_0 / \varepsilon\varepsilon_0}$.

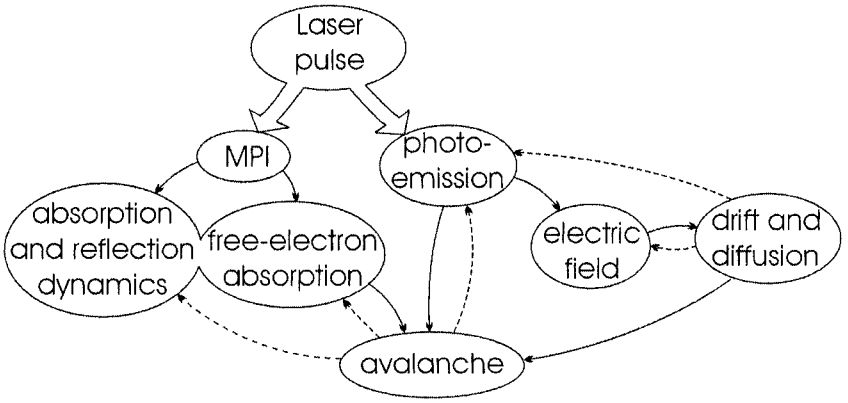

Figure 2. Modeling scheme. Major interconnections between different processes are shown by the arrows. Direct effects are indicated by solid lines and feedback effects are shown with dashed lines.

4. CARRIER DYNAMICS AND MODELING APPROACHES TO CARRIER TRANSPORT

The importance of carrier dynamics under pulsed laser ablation (PLA) conditions, especially for ultrashort laser pulses, has been demonstrated in numerous studies (Petite, et al., 1996; Li, et al., 1999; Stoian, et al., 2002b). Electronic transport differs strongly in various classes of materials irradiated under similar conditions at moderate energy densities (Stoian, et al., 2002a; Bulgakova, et al., 2004a). We discuss a situation where, apart from the

photoemission yield, the mobility of the charge carriers, electrons and holes, is the main parameter influencing the rate of charge redistribution in self-consistent electric fields generated under the action of pulsed laser radiation. Mobility determines both drift and diffusion of charge carriers, including thermal diffusion in the presence of temperature gradients.

The theoretical description of carrier dynamics in dielectric and semiconductor targets under short pulsed laser irradiation is a complicated task which implies consideration of a broad spectrum of interrelated processes. A simplified scheme of the processes triggered by ultrafast laser irradiation in dielectrics and semiconductors is shown in Fig. 2. A laser pulse impinging on a target causes photoionization (with the order of the process depending on the relation between the photon energy and the material energy band-gap) and photoemission (with the order of nonlinearity determined by the ratio of the work function to the photon energy). The electrons excited to the conduction band absorb further laser radiation and can produce secondary electrons by collisional ionization. In addition, they change the dielectric response of the material, thus explicitly influencing the optical properties. As soon as electronic avalanche is developed, absorption and reflection dynamics vary dramatically. Photoemission depletes a superficial target layer arresting further development of collisional multiplication and, in turn, avalanche regulates photoemission through its influence on the available free-electron density. Another drastic consequence of electron photoemission is the violation of the target quasi-neutrality that results in positive charging of the target as a whole and thus in generation of an ambipolar electric field. The electric field forces the charge carriers to relocate in order to neutralize the excess positive charge. The electric current is a superposition of two components: charge-carrier drift in the electric field and diffusion under the action of the gradients, both in density and temperature. Redistribution of free electrons due to the electric current strongly influences both electron photoemission and the avalanche multiplication process.

Existing models treat most, or at least some, of the processes described above and may, by convention, be divided into three groups. One of the dominating approaches to describe carrier dynamics in silicon targets is based on ambipolar diffusion with an implicit assumption of an equal number of electrons and holes in the solid and the preservation of local quasi-neutrality of the sample (Yoffa, 1980; van Driel, 1987; Mao, et al., 1998). Another group of models, developed for semiconductors irradiated by laser pulses (Held, et al., 1991) and dielectrics under the action of electron beams (Melchinger and Hofmann, 1995; Miotello and Dapor, 1997), takes into account the generation of local electric fields inside the target with the assumption that the target remains neutral as a whole. This implies the absence of electron photoemission (Held, et al., 1991) or relies on secondary electron emission equal to the absorbed electron flux (Melchinger and

Hofmann, 1995; Miotello and Dapor, 1997). In this approach, the concept of a double layer can be applied to describe the spatial charge arrangement in the bulk of the irradiated materials (Melchinger and Hofmann, 1995).

A third approach (Ribeiro, et al., 1997, 1998), proposed for the case of a dielectric target (MgO) irradiated by a laser pulse of nanosecond duration, may be labeled as the drift-diffusion approach. The authors studied the self-consistent generation of an electric field as a result of laser heating and thermionic emission of the electrons excited to the conduction band and their diffusion and drift in the locally established fields. It was found that the self-consistent electric field could reach values exceeding 10^8 V/m under normal ablation conditions. In several recent works (Stoian, et al., 2002a, Bulgakova, et al., 2004a, 2004b, 2005a, 2005b) the authors used the same simplified approach to model charging of different types of materials under ultrashort pulsed laser irradiation, taking into account specific properties of the materials. This implies calculations of energy deposition into the electronic subsystem and subsequent heating of the lattice through electron-lattice energy exchange. For the latter task we used the two-temperature model which is mostly utilized to describe metals heated by ultrashort laser pulses (Kaganov, et al., 1957; Anisimov, et al., 1974; Wellershoff, et al., 1999).

5. A UNIFIED APPROACH

Under high power ultrafast laser irradiation, dense plasmas are generated in dielectrics and semiconductors (Stuart, et al., 1996; Tien, et al., 1999; Nolte, et al., 1999; Sokolowski-Tinten and von der Linde, 2000), thus justifying a unified approach based on an intrinsic or a laser-induced metallic behavior for the three classes of materials investigated. The following equations are used as the building blocks for a common simplified frame applicable to different kinds of materials:

(1) The continuity equations for the evolution of the laser-generated charge carriers:

$$\frac{\partial n_x}{\partial t} + \frac{1}{e}\frac{\partial J_x}{\partial x} = S_x + L_x, \qquad (1)$$

where S_x and L_x are the source and loss terms describing the free carrier populations, n_x denotes the carrier densities, with subscript $x = e, i$ representing electrons and ions, respectively;

(2) The expression for the electric current density J_x includes drift and diffusion terms (Ribeiro, et al., 1998) and can be considered as the equation of motion:

$$J_x = |e| n_x \mu_x E - e D_x \nabla n_x . \qquad (2)$$

Here the time and space dependent diffusion coefficient D_x is calculated according to the Einstein relation as $D_x = kT_x\mu_x/e$, where T_x represents the carrier temperature, k is the Boltzmann constant, and μ_x is the carrier mobility. We assume that the charge-carrier flows are caused by quasi-neutrality violation on and below the target surface due to electron photoemission and strong density and temperature gradients.

(3) Poisson equation to calculate the electric field generated as a result of breaking quasi-neutrality in the irradiated target:

$$\frac{\partial E}{\partial x} = \frac{e}{\varepsilon\varepsilon_0}\left(n_i - n_e\right) . \qquad (3)$$

(4) Energy conservation equations to account for the heating of electronic and lattice subsystems. We assume that laser-excited metals and strongly ionized insulators and semiconductors can be considered as dense plasmas so that the two-temperature model (Kaganov, et al., 1957; Anisimov, et al., 1974; Wellershoff, et al., 1999) may be applied for the description of the energy balance:

$$C_e\left(\frac{\partial T_e}{\partial t} + \frac{J}{en_e}\frac{\partial T_e}{\partial x}\right) = \frac{\partial}{\partial x} K_e \frac{\partial T_e}{\partial x} - g(T_e - T_l) + \Sigma(x,t) \qquad (4)$$

$$(C_l + L_m \delta(T_l - T_m))\frac{\partial T_l}{\partial t} = \frac{\partial}{\partial x} K_l \frac{\partial T_l}{\partial x} + g(T_e - T_l) . \qquad (5)$$

Even if complete equilibration does not take place in the subsystems, the values T_e and T_i can be considered as measures for the average energies of electrons and lattice. In the Equations (4) and (5), indexes e, l refer to the electron and lattice parameters; C_e, C_l, K_e, K_l are the heat capacities and the thermal conductivities of electrons and lattice respectively; g is the electron-lattice coupling constant; and $\Sigma(x,t)$ is the energy source term. All these parameters will be specified below for every type of material. The term $L_m\delta(T - T_m)$ allows calculations of the liquid–solid interface (Zvavyi and Ivlev, 1996) having the temperature T_m, where L_m is the latent heat of fusion. The electron energy equation accounts for both heat conductivity and direct bulk or across the vacuum interface electronic transport (e.g. due to photoemission).

The system of equations (1)–(5) was solved numerically for targets irradiated with a laser pulse having a Gaussian temporal profile. The calculations were performed for a laser radiation wavelength $\lambda = 800$ nm and a pulse duration of $\tau_L = 100$ fs (FWHM) (Stoian, et al., 2000c, 2002a). A one-dimensional model, justified by the much larger transverse lateral dimensions for the laser spot compared to the absorption depth, has been employed. Particular situations for each class of material will be discussed below.

5.1 Metals

The continuity equation for free electrons (Eq. (1)) in a metal target (gold in our case) has no source terms. Photoemission was considered in the form of a surface boundary condition for the electron current density (Logothetis and Hartman, 1969; Bechtel, et al., 1977), describing electron flow into the vacuum. The three-photon photoemission cross-section c was determined empirically (Logothetis and Hartman, 1969) and was corrected here for the 800 nm irradiation wavelength. Ultrafast, sub-ps irradiation of metals can induce high electronic temperatures, ~1 eV, while the lattice remains cold during the irradiation time. Assuming temperature-dependent effects, we corrected the photoemission cross-section, based on the generalized Fowler-DuBridge theory for multiphoton photoemission at high temperatures (Bulgakova, et al., 2004a). The thermal emission of high-temperature electrons can also play a significant role. Thus, the photoemission term is written in the form:

$$J_s = c\frac{2(kT_e)^2}{(3\hbar\omega-\varphi)^2}F\left(\frac{3\hbar\omega-\varphi}{kT_e}\right)(1-R)^3 I^3 + A_0 T_e^2 \exp\left(-\frac{e\varphi}{kT_e}\right). \qquad (6)$$

Here A_0 is the Richardson coefficient, φ is the work function [4.25 eV (Samsonov, 1965)], $\hbar\omega$ is the incident photon energy (1.55 eV), and F is the Fowler function (Bechtel, et al., 1977).

The parameters for the energy equations (4)-(5) for gold are similar to the parameters reported by Wellershoff, et al. (1999), as well as the energy source accounting for ballistic effects of electronic energy transport. Optical properties for gold are taken for 800 nm wavelength. Electron mobility was estimated from data on gold conductivity (Grigoryev, et al., 1996) and found to be $5.17 \cdot 10^{-3}$ m^2/(V·s).

5.2 Dielectrics

In dielectric materials, free electrons are generated in the processes of multiphoton (MPI) and collisional ionization, and their recombination usually proceeds through a trapping-like phenomenon. For sapphire as an example, the source and loss terms in Eq. (1) for electrons can be written as:

$$S_e = (W_{\text{mph}} + Q_{\text{av}})\frac{n_a}{n_a + n_i}, \quad L_e = -R_e - PE. \tag{7}$$

Here $W_{\text{mph}}=\sigma_6 I^6$ is the rate of a 6-photon ionization process corresponding to an energy forbidden band E_g of ~9 eV, n_a is the density of neutral atoms, $Q_{\text{av}}=\alpha I n_e$ is the avalanche term (Stuart, et al., 1996), R_e represents the decay term taken in the form n_e/τ with τ = 1 ps, and PE denotes photoelectron emission. To compensate for the mobility decay with temperature, we use a simplified, time-independent diffusion coefficient, assuming that the average electron energy in the conduction band is ~5 eV (Arnold and Cartier, 1992; Stuart et al., 1996). The values of $\sigma_6 = 8\cdot10^9$ cm^{-3}ps^{-1}(cm^2/TW)^6 and $\alpha = 6$ cm^2/J were estimated by fitting the experimental determination of the optical damage threshold at different pulse durations (Ashkenasi, et al., 2000).

Attenuation of the laser power inside the dielectric target is determined by loss mechanisms involving free electron generation and by the optical response of a free-electron plasma through the Fresnel formulas. The complex dielectric function can be seen as a mutual contribution of the unexcited solid and the response of the laser–induced free electron gas (Driscoll and Vaughan, 1978; Sokolowski-Tinten and von der Linde, 2000). The local intensity $I(x,t)$ is given by the superposition of the direct irradiation and back-scattered radiation:

$$\frac{\partial}{\partial x} I(x,t) = -W_{\text{mph}} \frac{n_a}{(n_a + n_i)} \hbar\omega n_{\text{ph}} - a_{\text{ab}}(x,t) I(x,t) . \tag{8}$$

Here n_{ph} is the number of photons required for a MPI event (n_{ph} = 6). The free electron absorption coefficient $a_{\text{ab}}(x,t)$ is calculated from the complex dielectric response (Stuart, et al., 1996).

For a quantitative estimation of photoemission, we assume a statistical distribution of free electronic momenta in a wide bandgap dielectric where the vacuum level lies close to the conduction band minimum, and only electrons with a momentum component normal to and in the direction of the surface can escape into the vacuum. Thus, we assume that, on average, half of the electrons generated in the MPI and avalanche processes are emitted from the target. Maximum photoemission occurs from the surface with an

exponentially decreasing probability with bulk depth (Bulgakova, et al., 2004a):

$$PE(x,t)=\frac{1}{2}\left(W_{\text{mph}}+Q_{\text{av}}\right)\frac{n_a}{n_a+n_i}\exp(-x/l_{PE}) \qquad (9)$$

where the electronic escape depth l_{PE} is 1 nm (Jones, et al., 1988). The integral photoemitted charge calculated as above is in good agreement with reported experimental values for dielectric materials (Siekhaus, et al., 1986).

The ion density is calculated based on Eq. (1), disregarding photoemission and neglecting hole transport in the bulk. The electron mobility is taken as $\mu_e = 3\cdot10^{-5}$ m^2/(V·s) (ten times lower than reported by Hughes, 1979) for a better match of the observed diffusivities (Miotello and Dapor, 1997) in laser-induced dense plasmas. The source term in the energy equation (4) was constructed to account for the energy of the electrons generated via photoionization, energy expenses for avalanche multiplication, free electron absorption, and the energy localized in the strained lattice via trapping processes (Bulgakova, et al., 2005a). The thermodynamic parameters for the electronic subsystem were taken according to van Driel (1987). The value g can be defined via the characteristic electron-lattice relaxation time τ_r as $g = C_e/\tau_r$ ($\tau_r \sim 1$ ps).

5.3 Semiconductors

The model for silicon is based on a similar approach as for sapphire. The reflection of radiation at the vacuum interface and light absorption inside the bulk of a strongly excited semiconductor are described based on the mutual contribution of the unexcited material and the Drude response of the laser-generated free electron gas (Sokolowski-Tinten and von der Linde, 2000). In Eq. (1), one and two-photon ionization terms and avalanche were considered (Mao, et al., 1998; Sokolowski-Tinten and von der Linde, 2000):

$$S_e=\left[\left(\sigma_1+\frac{1}{2}\sigma_2 I\right)\frac{I}{\hbar\omega}+\delta n_e\right]\frac{n_a}{n_a+n_i}, \qquad L_e=-R_e-PE \qquad (10)$$

where σ_1 and σ_2 are one- and two-photon ionization cross-sections [σ_1 = 1021 cm^{-1} (Choi and Grigoropoulos, 2002), σ_2 = 10 cm/GW (Sjodin, et al. 1998)], the total atomic density is $n_0 = (n_a + n_i) = 5\cdot10^{22}$ cm^{-3}, and δ is the avalanche coefficient (van Driel, 1987). The loss term at low electronic densities is mainly determined by Auger recombination which saturates at electronic densities approaching 10^{21} cm^{-3} (Bok and Combescot, 1981). Consequently, the decay rate can be written as $R_e = n_e/(\tau_0 + 1/Cn_e n_i)$, with

$\tau_0 = 6 \cdot 10^{-12}$ s and $C = 3.8 \cdot 10^{-31}$ cm^6/s (van Driel, 1987). The equation for hole generation takes into account the hole transport process. The mobilities for electrons and holes are taken to be (Kuhn and Mahler, 1989) $\mu_e = 0.015$ m^2/(V·s) and $\mu_h = 0.0045$ m^2/(V·s), ten times reduced compared to the low electron-hole density values (Hummel, 1993). Diffusion coefficients for electrons and holes are calculated according to the Einstein relation.

Electron photoemission (Kane, 1962) was considered in analogy with gold [Eq. (6)] taking into account a three-photon photoemission from the conduction band with a coefficient corrected for the wavelength and the accessible density of states (Bulgakova, et al., 2004a). Instead of the Si work function ($\varphi = 4.6$ eV), an effective potential barrier $\varphi_{\text{eff}} = 4.05$ eV measured from the bottom of the conduction band (Mihaychuk, 1999) was introduced as the relevant parameter for the Fowler function.

The spatial and temporal distribution of the laser intensity in the sample was calculated taking into account one- and two-photon ionization, and free-electron absorption of the light. The source term for the heat transport equation (4) was calculated considering the balance of the laser energy deposited in the free electronic system (Bulgakova, et al., 2005a). The electron-lattice relaxation time was taken as $\tau_T = \tau_R(1 + (n_e/n_{cr})^2)$ with $\tau_R =$ 240 fs (Sjodin, et al. 1998).

6. RESULTS AND DISCUSSION

The model was first tested by calculating the damage thresholds for Au, Si, and Al_2O_3 and comparing them with previously published data on laser melting and damage of thin gold films (Wellershoff, et al., 1999) and optical breakdown in sapphire and silicon (Li, et al., 1999; Ashkenasi, et al., 2000; Cavalleri, et al., 2001). The results of the modeling are in good agreement with experimental observations (Bulgakova, et al., 2005a).

In Figure 3 the temporal profiles of the net positive charge resident on the surface for samples representative of different classes of materials (Al_2O_3, Si, and Au) are plotted for laser pulses of 100 fs duration at 800 nm wavelength. The laser fluences are chosen to be slightly above the experimental ion emission thresholds (Wellershoff, et al., 1999; Li et al., 1999; Quèrè, et al., 1999; Ashkenasi, et al., 2000; Sokolowski-Tinten and von der Linde, 2000), namely 4, 0.8, and 1.2 J/cm^2 for sapphire, silicon, and gold respectively. Under these specific irradiation conditions the electronic temperature reaches values ranging from around 1 eV in gold, to approximately 6 eV in silicon and more than 10 eV in sapphire. It is obvious that the net charge is significantly higher for the dielectrics than for the metal or for the semiconductor target.

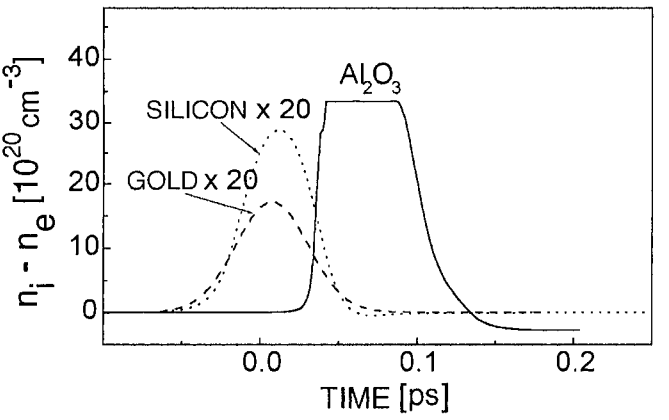

Figure 3. Temporal behavior of the net surface charge density (the difference between the hole and electron populations) for different classes of materials. Laser fluences are chosen to be above the ion emission threshold for each material (4 J/cm^2, 0.8 J/cm^2, and 1.2 J/cm^2 for Al_2O_3, Si, and Au, respectively). The laser pulse of 100 fs duration is centered at $t = 0$.

It should be emphasized that strong charging of sapphire (Fig. 3) is not a result of higher photoemission as compared to silicon and gold. According to modeling, the photoemission yield is approximately $6.8 \cdot 10^8$ electrons for the sapphire target over the whole laser pulse duration from an irradiated spot of 470 μm^2, whereas $6.2 \cdot 10^{11}$ and $3.5 \cdot 10^{11}$ electrons are removed for Si and Au targets, respectively. At the same time, the largest electric field is generated in the sapphire target. Figure 4 shows the temporal behavior of the electric field developed at the sapphire surface in comparison with the fields induced in other types of materials. The electric field exceeds the critical value and reaches a value of $8.4 \cdot 10^{10}$ V/m beneath the surface. The above threshold electric field exists for a few tens of fs. The spatial distribution of the electric field in the near-surface layers is given in Fig. 5 for times when the generated electric field is at its maximum. For sapphire, the layer with overcritical electric field where electrostatic disintegration of the lattice should occur is approximately 40 Å wide, in excellent agreement with the experimental estimation of the Coulomb exploded region (Stoian, et al., 2000c).

As discussed above, the electric field in the first cell below the surface reaches the value of ~8.4×10^{10} V/m for sapphire. An external field $E_{ex}=\varepsilon E_{in}$ is established in front of the surface, with ε being the relative permittivity. The accumulated electrostatic stress determines the surface disruption and the emitted Al^+ ions will be driven by the field for about a few tens of fs

(characteristic time of the electric field "pulse" in Fig. 4), and subsequently accelerated.

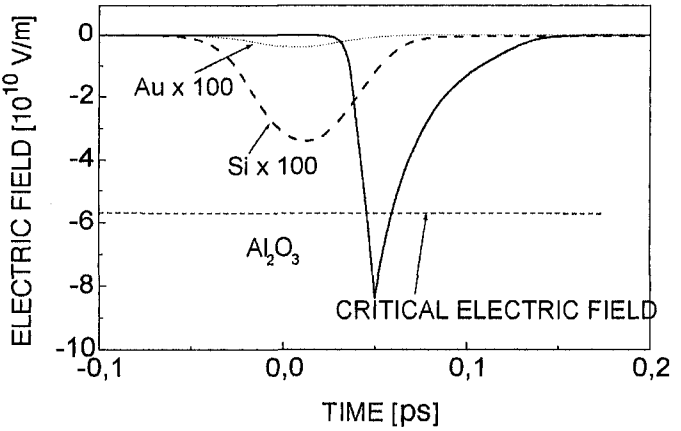

Figure 4. Temporal profiles of the laser-induced electric field at the surface region of the targets. Irradiation conditions as in Fig. 3.

The final momentum obtained by the ions subject to the action of the electric field E_{ex}, during time τ, is written as $m_{Al} \cdot v = eE_{ex}\tau$, where m_{Al} is the ion mass. This gives an estimate of the maximum velocity acquired by the ion of $v \geq 10^4$ m/s that closely agrees with the value detected in the time-of-flight experiments (Stoian, et al., 2000c). During the time of considerable surface charging, the ions travel a distance of the order of a few tens of Å. Thus, the charged surface layer is destroyed within an interval of several tens of femtoseconds.

With semiconductors and metals, the higher electron mobility and higher density of free electrons ensure effective screening and a much smaller net positive charge accumulated during the laser pulse, in spite of the fact that for the Si sample, supercritical carrier densities are reached. This is not sufficient to induce a macroscopic electrostatic breakup of the outer layers of the substrate. The maximum values of the electric field are only 4.1×10^7 V/m and 3.4×10^8 V/m for gold and silicon, respectively (Figs. 4 and 5).

We note here that recent studies (Roeterdink, et al., 2003) have indicated the emission of energetic ions for high-fluence irradiated silicon. The possible electrostatic mechanisms of ion ejection from laser-exposed regions where ultrafast phase-transitions (to transient states with low carrier transport properties) occur are not discussed in this work.

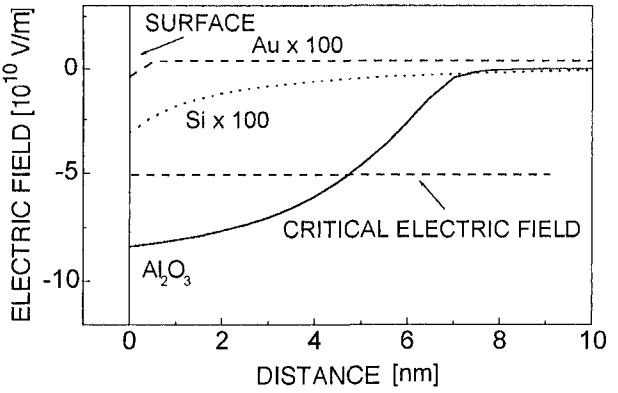

Figure 5. Spatial bulk profiles of the electric field induced by ultrafast laser radiation in metals, semiconductors, and dielectrics at time moments corresponding to the maximum values of the electric field for each material.

The charge dynamics are strongly correlated with the absorption characteristics for each material (see Fig. 3). In the case of sapphire, the charge maximum is strongly retarded, instead of roughly following the laser pulse envelope, as for metals and semiconductors. The effect is explained by the fact that electron heating and collisional multiplication take place during the tail of the laser pulse, thus being directly linked to the number of free electrons in the surface layers. The calculations show that a sapphire sample irradiated by a laser pulse with a fluence of 4 J/cm^2, accumulates multiphoton-generated seed electrons during the first half of the pulse. Only when the electron density reaches a value of order of 10^{17}–10^{18} cm^{-3} does avalanche start to dominate over MPI that leads to the subsequent dielectric breakdown. At this point, very efficient electron heating and photoemission occurs, resulting in supercritical surface charging.

A mention should be made about spatial distributions of the accumulated charge in the near-surface regions for the sapphire target (Bulgakova et al., 2004a, 2005a). During the laser pulse and approximately 100 fs after the laser pulse termination, only a 50–60 Å thick surface layer is positively charged. Later the charging process reaches a quasi-equilibrium between the opponent drift and diffusion terms, with a slight variation in time due to possible electronic decay channels (recombination at traps, self-trapping, Auger recombination) and electron supply from the bulk. The surface layer acquires a negative net charge (Fig. 3) while a certain quantity of net positive charge still exists in the subsurface region. Due to the attraction generated by the narrow positive subsurface layer, a region with

electron excess arises in the less-ionized interface region, so the picture of a classic double layer develops similar to that generated at the boundary of expending plasmas (Bulgakova, et al., 2000).

7. CONCLUSIONS

We have reviewed a unified continuum approach to describe the electronic transport in materials of different classes under the action of pulsed laser radiation. The approach is applied to model the charging of metallic, dielectric, and semiconductor targets irradiated by femtosecond, *near-infrared* laser pulses at intensities slightly above the material removal threshold. For dielectrics (sapphire as an example) the laser irradiation induces conditions for the electrostatic explosion of the target surface layer, in good agreement with the experimental observations (Stoian, et al., 2000c). This effect appears to be strongly inhibited for metals and semiconductors in the studied conditions as a consequence of their superior carrier transport properties.

The model can be applied to any material by taking into consideration the particular material properties. The model can also be applied for other irradiation conditions. Thus, for ultraviolet laser pulses, it has been recently shown that the Coulomb explosion mechanism can also be induced in silicon for nanosecond irradiation regimes while, for fs, UV pulses, phase explosion is the dominant process from the onset of ablation (Marine, et al., 2004; Bulgakova, et al., 2005a). However, a quantification of the Coulomb explosion behavior of silicon calls for further studies in view of uncertainties in the photoemission efficiency (Bulgakova, et al., 2005a).

Another intriguing aspect is the possibility of Coulomb explosion in conductors or semiconductors exposed to high laser fluences. It has been argued that an electric field sufficient for electrostatic disintegration of the crystalline lattice can be generated even for metals under extremely high laser fluences (Borghesi, et al., 2003). At moderate laser fluences, Coulomb explosion of dielectrics can be realized on a fs-time scale preceding the volume ablation via thermal mechanisms involving phase transitions. In this case, the observed ion energies are found to change from highly energetic non-thermal to thermal distributions (Stoian, et al., 2000c). However, under high laser fluences, strong gradients of the electron density considerably reduce the possibility to apply continuum approaches. Other formal schemes, e.g. combinations of the continuum approach for generation of free-carriers and electric field with the Boltzmann equation for the electronic transport, and energy relaxation in the electron subsystem, are desirable.

REFERENCES

Anisimov, S. I., Kapeliovich, B. L., and Perel'man, T. L., 1974, Electron emission from metal surfaces exposed to ultrashort laser pulses, *Sov. Phys. JETP*, **39**: 375-377.

Arnold, D., and Cartier, E., 1992, Theory of laser-induced free-electron heating and impact ionization in wide-ban-gap solids, *Phys. Rev. B* **46**:15102-15115.

Ashkenasi, D., Rosenfeld, A., Varel, H., Wärmer, M., and Campbell, E. E. B., 1997, Laser processing of sapphire with picosecond and subpicosecond pulses, *Appl. Surf. Sci.* **120**:65–80.

Ashkenasi, D., Stoian, R., and Rosenfeld, A., 2000, Single and multiple ultrashort laser pulse threshold of Al_2O_3 (corundum) at different etch phases, *Appl. Surf. Sci.* **154-155**:40-46.

Bechtel, J. H., Lee Smith, W., and Bloembergen, N., 1977, Two-photon photoemission from metals induced by picosecond laser pulses, *Phys. Rev. B* **15**:4557-4563.

Bitenskii, L. S., Murakhmetov, M. N., and Parilis, É. S., 1979, Sputtering of nonmetals by intermediate-energy multiply charged ions through a Coulomb "explosion", *Sov. Phys. Tech. Phys.* **24**:618-620.

Bok, J., and Combescot, M., 1981, Comment on the "Evidence for a self-confined plasma" in laser annealing, *Phys. Rev. Lett.* **47**:1564.

Borghesi, M., Romagnani, L., Schiavi, A., Campbell, D. H., Haines, M. G., Willi, O., Mackinnon, A. J., Galimberti, M., Gizzi, L., Clarke, R. J., and Hawkes, S., 2003, Measurement of highly transient electrical charging following high-intensity laser-solid interaction, *Appl. Phys. Lett.* **82**:1529-1531.

Brand, J.L., and Tam, A.C., 1990, Mechanism of picosecond ultraviolet-laser sputtering of sapphire at 266 nm, *Appl. Phys. Lett.* **56**:883-885.

Bulgakova, N. M., Bulgakov, A. V., and Bobrenok, O.F., 2000, Double layer effects in laser-ablation plasma plumes, *Phys. Rev. E* **62**:5624-5635.

Bulgakova, N. M., Stoian, R., Rosenfeld, A., Hertel, I. V., and Campbell, E. E. B., 2004a, Electronic transport and consequences for material removal in ultrafast pulsed laser ablation of materials, *Phys. Rev. B*, **69**:054102(1-12).

Bulgakova, N. M., Stoian, R., Rosenfeld, A., Campbell, E. E. B., and Hertel, I. V., 2004b, Model description of surface charging during ultra-fast pulsed laser ablation of materials, *Appl. Phys. A* **79**:1153-1155.

Bulgakova, N. M., Stoian, R., Rosenfeld, A., Hertel, I. V., Marine, W., and Campbell, E. E. B., 2005a, A general continuum approach to describe fast electronic transport in pulsed laser irradiated materials: The problem of Coulomb explosion, , *Appl. Phys. A* **81**:345-356.

Bulgakova, N. M., Stoian, R., Rosenfeld, A., Hertel, I. V., and Campbell, E. E. B., 2005b, Surface charging under pulsed laser ablation of solids and its consequences: studies with a continuum approach, *Proc. SPIE* **5714**:9-23.

Cavalleri, A., Siders, C. W., Rose-Petruck, C., Jimenez, R., Tóth, Cs., Squier, J. A., Barty, C. P. J., and Wilson, K. R., 2001, Ultrafast x-ray measurement of laser heating in semiconductors: Parameters determining the melting threshold, *Phys. Rev. B* 63:193306 (1-4).

Cheng, H.-P., and Gillaspy, J. D., 1997, Nanoscale modification of silicon surfaces via Coulomb explosion, *Phys. Rev. B* **55**:2628-2636.

Choi, T. Y., and Grigoropoulos, C. P., 2002 Plasma and ablation dynamics in ultrafast laser processing of crystalline silicon, *J. Appl. Phys.* **92**: 4918-4925.

Costache, F., Henyk, M., and Reif, J., 2003, Surface patterning on insulators upon femtosecond laser ablation, *Appl. Surf. Sci.* **208–209**:486–491.

Costache, F., and Reif, J., 2004, Femtosecond laser induced Coulomb explosion from calcium fluoride, *Thin Solid Films* **453-454**:334-339.

Dong, Y., and Molian, P., 2004, Coulomb explosion-induced formation of highly oriented nanoparticles on thin films of 3C-SiC by the femtosecond pulsed laser, *Appl. Phys. Lett.* **84**:10-12.

van Driel, H.M., 1987, Kinetics of high-density plasmas generated in Si by 1.06-and 0.53 μm picosecond laser pulses, *Phys. Rev. B* **35**:8166-8176.

Driscoll, W. G., and Vaughan, W., (Eds), 1978, *Handbook of Optics*, McGraw-Hill Book Company, New York.

Drits, M.E., (Ed.), *Properties of Elements: Handbook* (Moscow, Metallurgiya, 1985) (in Russian).

Fleischer, R. L., Price, P. B., and Walker, R. M., 1965, Ion explosion spike mechanism for formation of charged-particle tracks in solids, *J. Appl. Phys.* **36**:3645-3652.

Gamaly, E. G., Rode, A. V., Luther-Davies, B., and Tikhonchuk, V. T., 2002, Ablation of solids by femtosecond lasers: Ablation mechanism and ablation thresholds for metals and dielectrics, *Phys. Plasmas* **9**:949-957.

Grigoryev, I. S., Meilikhov, and E. Z., Radzig, A.A., (Eds), 1996, *Handbook of Physical Quantities*, CRC Press, Boca Raton, FL.

Held, T., Kuhn, T., and Mahler, G., 1991, Influence of internal electric fields and surface charges on the transport of an optically generated electron-hole plasma, *Phys. Rev. B* **44**: 12873-12879.

Henyk, M., Mitzner, R., Wolfframm, D., and Reif, J., 2000a, Laser-induced ion emission from dielectrics, *Appl. Surf. Sci.* **154-155**:249-255.

Henyk, M., Wolfframm, D., and Reif, J., 2000b, Ultra short laser pulse induced charged particle emission from wide bandgap crystals, *Appl. Surf. Sci.* **168**:263-266.

Herrmann, R., Gerlach, J., and Campbell, E. E. B., 1998, Ultrashort pulse laser ablation of silicon: an MD simulation study, *Appl. Phys. A* **66**(1):35-42.

Hughes, R.C., 1979, Generation, transport, and trapping of excess charge carriers in Czochralski-grown sapphire, *Phys. Rev. B* **19**:5318-5328.

Hummel, R. E., 1993, *Electronic Properties of Materials*, Springer-Verlag, Berlin, Heidelberg.

Jones, S. C., Fischer, A. H., Braunlich, P., and Kelly, P., 1988, Prebreakdown energy absorption from intense laser pulses at 532 nm in NaCl, *Phys. Rev. B* **37**:755-770.

Kaganov, M. I., Lifshitz., I. M., and Tanatarov, M. V., 1957, Relaxation between electrons and crystalline lattices, *Sov.Phys. JETP* **4**:173-178.

Kanasaki, J., and Tanimura, K., 2002, Laser-induced electronic desorption of Si atoms from Si(111)-(7×7), *Phys. Rev. B* **66**:125320(1-5).

E.O. Kane, 1962, Theory of photoelectric photoemission from semiconductors", *Phys. Rev.* **127**:131-141.

Kuhn, T., and Mahler, G., 1989, Carrier capture in quantum wells and its importance for ambipolar transport, *Solid-State Electron.* **32**:1851-1855.

Li, M., Menon, S., Nibarger, J. P., and Gibson, G.N., 1999, Ultrafast electron dynamics in femtosecond optical breakdown of dielectrics, *Phys. Rev. Lett.* **82**:2394-2397.

Logothetis, E. M., and Hartman, P. L., 1969, Laser-induced electron emission from solids: many-photon photoelectric effects and thermionic emission, *Phys. Rev.* **187**:460-474.

Mao, S. S., Mao, X.-L., Greif, R., and Russo, R.E., 1998, Simulation of infrared picosecond laser-induced electron emission from semiconductors, *Appl. Surf. Sci.* **127-129**:206-211.

Marine, W., Bulgakova, N. M., Patrone, L., Ozerov, I., 2004, Electronic mechanism of ion expulsion under UF nanosecond laser excitation of silicon: experiment and modeling, *Appl. Phys. A* **79**:771-774.

Mihaychuk, J. G., Shamir, N., and van Driel, H. M., 1999, Multiphoton photoemission and electric-field-induced optical second-harmonic generation as probes of charge transfer across the Si/SiO_2 interface, *Phys. Rev. B* **59**: 2164-2173.

Miotello, A., and Dapor, M., 1997, Slow electron impinging on dielectric solids. 2. Implantation profiles, electron mobility, and recombination processes, *Phys. Rev. B* **56**:2241-2247.

Melchinger, A., and Hofmann, S., 1995, Dynamic double-layer model description of time-dependent charging phenomena in insulators under electron-beam irradiation, *J. Appl. Phys.* **78**:6224-6232.

Nolte, S., Chichkov, B. N., Welling, H., Shani, Y., Lieberman, K., and Terkel, H., 1999, Nanostructuring with spatially localized femtosecond laser pulses, *Opt. Lett.* **24**,:914-916.

Petite, G., Daguzan, P., Guizard, S., and Martin, P., 1996, Conduction electrons in wide-bandgap oxides: a subpicosecond time-resolved optical study, *Nucl. Instr. Meth. B* **107**:97-101.

Quèrè, F., Guizard, S., Martin, P., Petite, G., Gobert, O., Meynadier, P., and Perdrix, M., 1999, Ultrafast carrier dynamics in laser-excited materials: subpicosecond optical studies, *Appl. Phys. B* **68**:459-463.

Ribeiro, R. M., Ramos, M. M. D., Stoneham, A. M., and Correia Pires, J. M., 1997, Modelling of surface evaporation by laser ablation, *Appl. Surf. Sci.* **109-110**:158-161.

Ribeiro, R. M., Ramos, M. M. D., and Stoneham, A. M., 1998, Mesoscopic modeling of laser ablation, *Thermophysics and Aeromechanics* **5**:223-234.

Roeterdink, W. G., Juurlink, L. B. F., Vaughan, O. P. H., Dura Diez, J., Bonn, M., and Kleyn, A.W., 2003 Coulomb explosion in femtosecond laser ablation of Si(111), *Appl. Phys. Lett.* **82**: 4190-4192.

Samsonov, G.V., (Ed.), 1965, *Physicochemical Properties of the Elements*, Naukova Dumka, Kiev (in Russian).

Schneider, D. H. G., and Briere, M. A., 1996, Investigations of the interactions of highest charge state ions with surfaces, *Phys. Scr.* **53**:228-242.

Siekhaus, W. J., Kinney, J. H., Milam, D., Chase, L. L., 1986, Electron emission from insulator and semiconducor surfaces by multiphoton excitation below the optical damage threshold, *Appl. Phys. A* **39**:163-166.

Sjodin, T., Petek, H., and Dai, H-L., 1998, Ultrafast carrier dynamics in silicon: a two-color transient reflection grating study on a (111) surface, *Phys. Rev. Lett.* **81**: 5664-5667.

Sokolowski-Tinten, K., and von der Linde, D., 2000, Generation of dense electron-hole plasmas in silicon, *Phys. Rev. B* **61**:2643-2650.

Stoian, R., Varel, H., Rosenfeld, A., Ashkenasi, D., Kelly, R., and Campbell, E. E. B., 2000a, Ion time-of-flight analysis of ultrashort pulsed laser-induced processing of Al_2O_3, *Appl. Surf. Sci.* **165**:44–55.

Stoian, R., Ashkenasi, D., Rosenfeld, A., Wittmann, M., Kelly, R., and Campbell, E. E. B., 2000b, The dynamics of ion expulsion in ultrashort pulse laser sputtering of Al_2O_3, *Nucl. Instrum. Methods Phys. Res. B* **166-167**:682-690.

Stoian, R., Ashkenasi, D., Rosenfeld, A., and Campbell, E. E. B., 2000c, Coulomb explosion in ultrashort pulsed laser ablation of Al_2O_3, *Phys. Rev. B* **62**(19):13167-13173.

Stoian, R., Rosenfeld, A., Ashkenasi, D., Hertel, I.V., Bulgakova, N.M., and Campbell, E. E. B., 2002a, Surface charging and impulsive ion ejection during ultrashort pulsed laser ablation, *Phys. Rev. Lett.* **88**:097603(1-4).

Stoian, R., Boyle, M., Thoss, A., Rosenfeld, A., Korn, G., Hertel, I. V., and Campbell, E. E. B., 2002b, Laser ablation of dielectrics with temporally shaped femtosecond pulses, *Appl. Phys. Lett.* **80**:353-355.

Stuart, B.C., Feit, M.D., Herman, S., Rubenchik, A.M., Shore, B.W., and Perry, M.D., 1996, Nanosecond-to-femtosecond laser-induced breakdown in dielectrics, *Phys. Rev. B* **53**:1749-1761.

Tam, A.C., Brand, J.L., Cheng, D.C., and Zapka, W., 1989, Picosecond laser sputtering of sapphire at 266 nm, *Appl. Phys. Lett.* **55**:2045-2047.

Tien, A.-C., Backus, S., Kapteyn, H., Murnane, M., and Mourou, G., 1999, Short-pulse laser damage in transparent materials as a function of pulse duration, *Phys. Rev. Lett.* **82**:3883-3886.

Vanagas, E., Kudryashov I, Tuzhilin D, Juodkazis, S., Matsuo, S., and Misawa, H., Surface nanostructuring of borosilicate glass by femtosecond nJ energy pulses, *Appl. Phys. Lett.* **82**(17):2901-2903.

Varel, H, Wähmer, M., Rosenfeld, A., Ashkenasi, D., and Campbell, E. E. B, 1998, Femtosecond laser ablation of sapphire: time-of-flight analysis of ablation plume, *Appl. Surf. Sci.* **127-129**:128-133.

Wellershoff, S.-S., Hohlfeld, J., Güdde, J., and Matthias, E., 1999, The role of electron-phonon coupling in femtosecond laser damage of metals, *Appl.Phys. A* **69**: S99-S107.

Yoffa, E.J., Dynamics of dense laser-induced plasmas, 1980, *Phys. Rev. B* **21**:2415-2425.

Zvavyi, S. P., and Ivlev, G. D., 1996, Influence of the initial silicon temperature on crystallization of a layer melted by nanosecond laser heating, *Inzh.-Fiz. Zh.* **69**:790-793 (in Russian).